Published in final edited form as:
Aging Cell. 2013 February ; 12(1): 167–176. doi:10.1111/acel.12033.

Alterations in Ventricular K_{ATP} Channel Properties during Aging

Li Bao, PhD[1], **Eylem Taskin, PhD**[1], **Monique Foster, BS**[1], **Beevash Ray, MD**[2], **Rosa Rosario**[2], **Radha Anathakrishnan, PhD**[2], **Susan Howlett, PhD**[3], **Ann Marie Schmidt, MD**[2], **Ravichandran Ramasamy, PhD**[2], and **William A. Coetzee, DSc**[1,3,4]

[1]Pediatrics, NYU School of Medicine, New York, NY

[2]Medicine, NYU School of Medicine, New York, NY

[3]Physiology & Neuroscience, NYU School of Medicine, New York, NY, Department of Pharmacology, Dalhousie University, 5850 College Street, PO Box 15000, Sir Charles Tupper Medical Building, Halifax, Nova Scotia, Canada B3H 4R2

[4]Pharmacology, NYU School of Medicine, New York, NY

Abstract

Coronary heart disease remains the principle cause of mortality in the United States. During aging, the efficiency of the cardiovascular system is decreased and the aged heart is less tolerant to ischemic injury. ATP-sensitive K^+ (K_{ATP}) channels protect the myocardium against ischemic damage. We investigated how aging affects cardiac K_{ATP} channels in the Fischer 344 rat model. Expression of K_{ATP} channel subunit mRNA and protein levels was unchanged in hearts from 26-month old vs. 4-month old rats. Interestingly, the mRNA expression of several other ion channels (>80) was also largely unchanged, suggesting that post-transcriptional regulatory mechanisms occur during aging. The whole-cell K_{ATP} channel current density was strongly diminished in ventricular myocytes from aged male rat hearts (also observed in aged C57BL/6 mouse myocytes). Experiments with isolated patches (inside-out configuration) demonstrated that the K_{ATP} channel unitary conductance was unchanged, but that the inhibitory effect of cytosolic ATP on channel activity was enhanced in the aged heart. The mean patch current was diminished, consistent with the whole-cell data. We incorporated these findings into an empirical model of the K_{ATP} channel and numerically simulated the effects of decreased cytosolic ATP levels on the human action potential. This analysis predicts lesser activation of K_{ATP} channels by metabolic impairment in the aged heart and a diminished action potential shortening. This study provides insights into the changes of K_{ATP} channels during aging and suggests that the protective role of these channels during ischemia is significantly compromised in the aged individual.

Keywords

K^+ Channels; K_{ATP} channel; Aging; numerical simulation; ischemia

Introduction

Aging is an inevitable event and is associated with declining health and an increased morbidity. In order to improve the quality of life, it is critical to understand the aging

Dr. William A. Coetzee NYU School of Medicine, Alexandria Center for Life Science 450 East 29th Street, floor 8 (824) New York, NY 10016, USA Tel: 1-646-501-4510 Fax: 1-212-263-5100 william.coetzee@nyu.edu.

Disclosures
None

process and the underlying causes responsible for the declining health. Cardiovascular disease is the leading cause of death in individuals over 65 (Fleg & Strait 2011). Their cardiac insufficiency is often associated with co-existing conditions like hypertension and diabetes. Nevertheless, intrinsic vascular and cardiac changes occur with age that may underlie age-related cardiovascular disease (Fleg JL 2008).

The K_{ATP} channel and protection against stress

K_{ATP} channels are comprised of pore-forming Kir6 subunits in combination with regulatory SUR subunits (Seino & Miki 2003). The Kir6 subunits (Kir6.1 and Kir6.2) determine the biophysical properties and nucleotide sensitivities of K_{ATP} channels while the SUR subunits (SUR1, SUR2A and SUR2B) fine-tune the nucleotide sensitivity and confer unique pharmacological specificities (Seino & Miki 2003). K_{ATP} channels are abundantly expressed in the cardiovascular tissues. They are weak inward rectifiers and are modulated by intracellular nucleotides, phosphoinositols, sulfonylureas and other pharmacological agents (Nichols 2006). By coupling tissue demand to electrical excitability, K_{ATP} channels have a protective role in cardiac pathophysiological states. Although much work has focused on the protective role of mitochondrial K_{ATP} channels, studies with K_{ATP} channel subunit deficient mice have demonstrated a clear protective role for sarcolemmal K_{ATP} channels during ischemia and ischemic preconditioning (Gross & Peart 2003).

Electrophysiological alterations associated with aging

Major age-related changes occur in the cardiac electrophysiological profile and in excitation-contraction coupling (Lakatta & Yin 1982; Howlett 2010). In humans and animal models the action potential is prolonged (Lakatta *et al.* 1975) and contractile responses are diminished (Rumberger & Timmermann 1976). These changes are associated with diminished activity of Na^+ channels and the L-type Ca^{2+} current (Rosen *et al.* 1978), the Na^+/K^+ pump (Poole *et al.* 1984), the transient outward K^+ current (Walker *et al.* 1993), pacemaker channels (Huang *et al.* 2007), and the inward rectifying K^+ current (Liu *et al.* 2000). The K_{ATP} channel is also subject to change during aging. In guinea-pig heart, a decreased K_{ATP} channel density has been described in middle-aged animals (Ranki *et al.* 2002). A more comprehensive analysis was performed in skeletal muscle from aged male rats (Tricarico & Camerino 1994), where additional features included an age-related decrease in open probability and a significantly enhanced (30-200 times) sensitivity to oxidation. The goal of this study was to perform an investigation of age-related changes in the cardiac K_{ATP} channel from aged rodents.

Methods

Animals

All animal handling procedures were in accordance with National Institutes of Health guidelines and were approved by the Institutional Animal Care and Use Committees of New York University School of Medicine. Fischer 344 young (5 months; 300±20g body weight) and aged (28-30 months; 438±18g) male rats were purchased from NIA colony (Bethesda, MD). In some studies, we also used young (4-6 months; 33.1±21.g) or aged (30 month old; 34.6±0.65) C57BL/6 male mice. Animals were free of tumors and other age-related morphological abnormalities at the time of use.

Isolation of ventricular myocytes

Single ventricular myocytes were isolated enzymatically. Following injection of heparin (500 IU/kg IP), rats were sacrificed with pentobarbital overdose (60 mg/kg body weight IP). The hearts were rapidly excised and placed in ice-cold Tyrode's buffer (in mM): NaCl 137,

KCl 5.4, HEPES 10, $MgCl_2$ 1, NaH_2PO_4 0.33, $CaCl_2$ 1.8; adjusted with NaOH to pH 7.4) prior to being retrogradely perfused through the aorta with Tyrode's buffer. The heart was then perfused for 3 min with nominally Ca^{2+}-free Tyrode's buffer for 3 min, followed by the same solution containing collagenase (3 mg/mL; Sigma C0130, type I) and protease (0.44 U/mL; Sigma, type XIV) for 11-13 min with young hearts and 17-20 min with aged hearts. Finally, the perfusion was switched for 3 min to KB solution (in mM: taurine 20, glutamate free acid 50, HEPES 10, EGTA [ethylene glycol-bis-([alpha]-aminoethyl ether) N,N,N',N'-tetra acetic acid] 0.5, $MgSO_4$ 3, KH_2PO_4 30, KCl 30, KOH 78; adjusted with KOH to pH 7.2). The ventricles were cut into small pieces (in KB solution) and teased apart with a disposable Pasteur pipette. Myocytes were filtered (150 μM mesh size) and allowed to settle in KB buffer for 1 hour at room temperature before experimentation (within 6h of isolation). The yield of rod shaped myocytes was >90% with young hearts and ~50% with aged hearts.

Whole-cell recordings

Isolated myocytes were plated on laminin-coated coverslips, mounted in a recording chamber (RC-21BRW, Warner Instruments) on the stage of an inverted microscope (Nikon TE2000-V, Morrell). Myocytes were continuously superfused with Tyrode's solution. Whole-cell membrane current was recorded at room temperature using standard patch-clamp techniques (Axopatch-200B amplifier, Axon Instruments) (Bao *et al.* 2011a). Patch pipettes were made using borosilicate glass (OD 1.5 mm) and had resistances between 1.5-3 MΩ when filled with a solution containing (mM): KCl 140; MgATP 0.1; MgADP 0.1; $MgCl_2$ 1; HEPES 10; and EGTA 1; titrated to pH 7.2 with KOH. . The Ca^{2+} activity in the pipette solution was calculated to be below 1nM. After gigaseal formation and patch rupture, whole-cell current was recorded at a holding potential of -45 mV. Current-voltage relationships were obtained using a ramp protocol (5mV to -100 mV at -25 $mV \cdot s^{-1}$, applied every 20s). Membrane currents were filtered (low-pass Bessel response with a cutoff frequency of –3 dB at 1 kHz), digitized at 5 kHz and stored on a computer hard disk with pCLAMP software (Clampex 9.0, Axon Instruments). No corrections were made for the liquid junction potential, which was calculated to be approximately 5mV.

Inside-out patch clamp recordings

Patch pipettes had resistances between 2-4 MΩ when filled with pipette solution (in mM) 150 KCl, 2 $CaCl_2$, 1 $MgCl_2$, and 10 HEPES, pH 7.4. The bath solution consisted of (mM) 150 KCl, 1 EGTA, 10 HEPES, 1.2 $MgCl_2$ and pH 7.2. Following patch excision, current was filtered (low-pass Bessel response with a cutoff frequency of -3 dB at 1 kHz), digitized at 5 kHz and stored on a computer hard disk with pCLAMP software (Clampex 9.0, Axon Instruments). Unless otherwise indicated, the pipette potential was +80mV (membrane potential of -80mV). Inward currents are represented as upward deflections in all figures. Solution exchanges were made using a rapid solution changer (RSC200, BioLogic SAS). Patches were exposed to 1 mM ATP at the beginning and the end of each experiment. These recordings were bracketed by recordings in zero ATP to ensure the absence of significant rundown. Rundown was corrected if needed. The K_{ATP} channel current (I/I_0) was calculated as the mean patch current (I) relative to the maximal current in the absence of ATP (I_0). ATP-inhibitory curves were obtained by fitting data to a sum of two pseudo-Hill functions (Origin 8, Originlab):

$$\frac{I}{I_O} = \frac{A1}{1+\left(\frac{[ATP]}{IC_{50}(1)}\right)^{h1}} + \frac{A2}{1+\left(\frac{[ATP]}{IC_{50}(2)}\right)^{h2}} \quad (1)$$

Where A1 and A2 the relative contributions (or weights) of the two components (with A1 + A2 = 1), $IC_{50}(1)$ and $IC_{50}(2)$ the concentration for half-maximal inhibition and h1 and h2 the respective Hill coefficients.

mRNA expression analysis

Animals were anesthetized and hearts were removed as described above (atria were discarded). Total RNA was extracted using the acid-phenol guanidinium method (TriReagent, Sigma) and the RNA quality was determined by agarose gel electrophoresis, assessed by intact 18S and 28S RNA bands. RNA concentrations were determined spectrophotometrically. Total RNA was reverse transcribed (Superscript III, Invitrogen) using a mixture of random hexamer primers and oligo-dT primers. Semi-quantitative real-time PCR was performed with SYBR green in triplicate in a 384-well format (ABI Prism 7900HT) and each well contained cDNA generated from 40 ng total RNA. The annealing temperature was 60°C and the number of cycles used was 40. The Ct values were determined (SDS software version 2.3, Applied Biosystems), corrected using a passive reference dye (Rox) present in the PCR master mix. Reactions with a Ct value larger than 36 or with any evidence of non-specificity (low melting temperatures or multiple peaks in melting point analysis) were excluded from the analysis. We calculated (as described(Harrell *et al.* 2007)) the target gene expression relative to that of reference genes, selected with the Normfinder algorithm(Andersen *et al.* 2004). Hierarchical clustering (Euclidian distance and complete linkage) was performed on log_2-transformed data and a heat map was produced (MEV v4.7.1). Significance Analysis of Microarrays (SAM) was performed with a delta value of 1.13 (90^{th} percentile false discovery rate of 8%). Conventional RT-PCR was performed to distinguish between SUR2A and SUR2B isoforms (Morrissey *et al.* 2005) (see **Table 1** for primers used).

Biochemistry methods

Membrane fractions from rat hearts were prepared using a modification of a previously described method (Bao *et al.* 2011a). In brief, hearts were flash frozen and ground to a fine powder (in liquid nitrogen) using a pestle and mortar. This was followed by homogenization with 30 strokes of a glass-glass homogenizer followed by 30 strokes in a Dounce homogenizer in (in mM) 250 sucrose, 1 EDTA, 10 HEPES, 1 DTT and pH 7.4 supplemented with protease inhibitor cocktail (Roche Applied Science). After a brief centrifugation (1,000 g for 5 min at 4°C), the supernatant was loaded on top of a 18% Optiprep (Sigma-Aldrich) layer (with in mM: 150 Sucrose, 1 EDTA, 10 HEPES and 1 DTT, pH 7.4, supplemented with protease inhibitor cocktail) and subjected to ultracentrifugation (250,000 g for 1 h at 4 °C). The membrane fraction was collected from the interphase and membranes were recovered by centrifugation (after dilution with 10 mM Tris/HCl, 1 mM EDTA, pH 7.5). The prepared membranes were resuspended in solubilization buffer (20 mM HEPES, pH 7.4 and 0.5% v/v Triton X100) at 4°C overnight. After removal of the insoluble material by centrifugation (10,000 g, 10 min, 4°C), protein concentration was determined (Bradford assay, Biorad) and samples were immediately used for immunoblotting experiments. Un-boiled proteins were resolved by 10% SDS-PAGE, transferred to PVDF membranes and blocked with 5% milk in TBS / 0.05% Tween for 1 hour. Primary and secondary antibodies dissolved in blocking buffer were incubated overnight at 4°C and 1 hour at room temperature respectively. Chemiluminescent Western blotting substrate (Pierce) was used for peroxidase detection and the resulting signal was detected on Kodak Biomax light films.

Primary antibodies used for Western blotting were: chicken anti-Kir6.2 (C62 developed by us (1: 2300), goat anti-SUR2A (Santa Cruz, 1:150), rabbit anti-SUR2B (rSUR2B, 1:300), rabbit anti-SUR1 (1:300). Secondary antibodies used were donkey anti-chicken-HRP

(703-035-155, Jackson, 1 :20,000, and donkey anti-goat-HRP (sc-2020, Santa Cruz Biotechnology; 1:10,000) and goat anti-rabbit-HRP (sc-2004, Santa Cruz Biotechnology; 1:20,000).

Numerical simulation

We used a numerical model of the ventricular K_{ATP} channel as described previously (Ferrero *et al.* 1996; Bao *et al.* 2011b). Full details of the models are available in the Supplementary information. In brief, the K_{ATP} channel current is expressed as:

$$I_{K,ATP} = N \times P_o \times \gamma \times f_{K,ATP} \times (E_m - E_K) \quad (2)$$

where $I_{K,ATP}$ the K_{ATP} channel current, N represents the channel density (channels/μm^2), P_o the intrinsic open probability in the absence of modulation by Na^+, Mg^{2+} and nucleotides, γ the unitary conductance (pS), $f_{K,ATP}$ the fraction of open channels, E_m the membrane potential (mV) and E_K the equilibrium potential for K^+ ions (mV).

Statistical Analysis

The mRNA levels in each subgroup of samples were characterized by their median values and ranges, standard error of the mean of individual reactions and their coefficients of variation. Differences between two samples were judged significant at confidence levels greater than 95% ($p < 0.05$). All other data are shown as mean ± SEM (*n* denoting the number of cells) and differences between groups were determined using appropriate tests as specified in the text (SigmaStat, Systat Software Inc), using a p-value of < 0.05.

Results

Action potential alterations with aging

Action potentials were recorded from ventricular cardiomyocytes enzymatically isolated from young and aged male Fischer 344 rats. **Figure 1** demonstrates that aging is associated with a significantly longer action potential duration, when recorded at 90% repolarization (55.1±8.4 vs 98±14.4ms in young and aged groups respectively, $p<0.05$). The action potential duration at 50% repolarization was also prolonged (23±4.3 in the young group vs 52±11.0 ms in the aged group, $p<0.05$), and there was a small, but not statistically significant, depolarization of the resting potential (-63±1.8mV in young group vs -58±2.4mV in the aged group). The action potential amplitude was not different between the two groups (respectively 96±4.7 and 90±5.7 mV in the young and aged groups). These data demonstrate that important alterations occur in the ionic currents underlying the normoxic action potential. Having established that the expected electrophysiological changes were observed in this animal model, our subsequent experiments were focused on investigating alterations of K_{ATP} channels with aging.

The K_{ATP} channel current density is lower in aged hearts

We next investigated alterations in membrane currents using whole-cell voltage clamp techniques (Bao *et al.* 2011a). There was no difference in the cell capacitance between the two groups, respectively 225±13.7 (n=16) and 215±19.2 pA (n=19) for young and aged rat ventricular myocytes. Current-voltage relationships (**Figure 1C**), obtained with ramp voltage pulses between -100 to 0mV, demonstrated smaller outward currents in the voltage range between -70 and -25 mV in ventricular myocytes isolated from aged hearts. K_{ATP} channels are not open under these normoxic conditions. We therefore activated K_{ATP} channel opening by inhibiting mitochondrial ATP production with dinitrophenol (DNP; 100 μM) (Bao *et al.* 2011a). **Figure 1D** demonstrates that the DNP-activated K_{ATP} channel

current density was significantly depressed in aged ventricular cardiomyocytes. For example, the DNP-activated current at -45mV was 43.3±6.15 pA/pF (n=19) in aged myocytes compared to 62.8±4.5 pA/pF (n=16; p=0.02, Student's t-test) in myocytes from young hearts. The DNP-activated current was sensitive to glibenclamide (2 μM), confirming its identity as the K_{ATP} channel current (**inset of Figure 1D**). In a parallel set of experiments, we also investigated effects of aging in mice, by comparing electrophysiological properties of ventricular myocytes isolated from young (4-6 month) and aged (30 month) C57BL/6 animals. Under normoxic conditions, the current-voltage relationship had a more pronounced outwardly rectifying component when compared to the rat (**Figure 1E**). Qualitatively, however, similar aging-dependent changes were observed in aged mouse myocytes. In mice, the effect of aging on DNP-activated K_{ATP} channel current density was even more pronounced than that in the rat (**Figure 1F**). For example, the DNP-activated current at -45mV was 17.5±2.16 pA/pF (n=14) in aged myocytes compared to 81.3±13.53 pA/pF (n=14; p<0.001, Mann-Whitney Rank Sum test) in myocytes from young hearts.

The nucleotide regulation of K_{ATP} channels

Next we used the inside-out patch clamp configuration to investigate K_{ATP} channels. The single channel conductance was 68.8±1.55 pS in aged rats versus 68.8±1.26 pS in young rats; p>0.05). We performed experiments to investigate the inhibition of K_{ATP} channels by ATP applied to the cytosolic face of the membrane. In the absence of ATP, the mean patch current was significantly smaller in patches isolated from aged Fischer 344 rat hearts when compared to young animals (83.5±3.37 pA, n=16 in the aged group vs. 164.3±16.11, n=20 in the young group; p=0.009, Mann-Whitney Rank sum test). As expected, the K_{ATP} channel current was progressively inhibited by elevating the cytosolic ATP concentrations between 0.1-1000 μM (**Figure 2A**). However, K_{ATP} channels from the aged heart were more sensitive to the inhibitory effect of ATP. This is apparent when inspecting the ATP-concentration curves, where half-maximal block occurred with ~30μM ATP in patches from the young hearts, compared to ~1-2uM ATP in the aged heart (**Figure 2B**). Curve fitting of the data to a modified Hill equation did not produce adequate results, particularly in the aged group (**Table 2; see also Supplemental Figure**). We therefore assumed a model where two ATP binding affinities (most likely originating from two separate populations of channels) contribute to the overall ATP sensitivity. Indeed, in the aged group a sum of two Hill equations adequately described the data, with IC_{50} values of 0.7 and 59.8 μM ATP (the Hill constants were respectively 1.3 and 1.5). Applying the same model to the young group also approximated the data better than fitting with a single Hill equation, with IC_{50} values of 1.7 and 74.5 μM ATP (the Hill constants were respectively 1.5 and 1.4). Although the IC_{50} values of the two components were similar between the two groups, their relative contributions (or weights) were different. In the young group, the low-affinity component contributed 66% towards the overall ATP-sensitivity curve, whereas its contribution was only 38% in the aged group, which resulted in the overall decrease in ATP-sensitivity.

Lack of transcriptional or translational regulation with aging

Given the significant alterations in K_{ATP} channel current density, we next investigated their transcriptional regulation in the aging rat heart. Using semi-quantitative real-time RT-PCR (primers are listed in **Table 1**), we compared the mRNA expression levels of K_{ATP} channel subunits in young and aged rat hearts (n=5 each) relative to that of β-actin (**Figure 3**). There were no significant differences between the two groups in mRNA expression of Kir6.1, Kir6.2, SUR1 or SUR2. Since the real-time RT-PCR experiment did not distinguish between SUR2 splice variants, we used conventional RT-PCR with a primer pair that produces a larger amplicon for SUR2A than for SUR2B(Morrissey *et al.* 2005; Bao *et al.* 2011b). This analysis demonstrates that there were no significant differences in SUR2A and SUR2B

splice variant mRNA expression between the young and aged rat ventricle. Prompted by the lack of transcriptional regulation on K_{ATP} channel subunit mRNA with aging, we extended the screen to evaluate the impact of sex and aging on 82 ion channel genes. A subset of the data is shown as a heatmap in **Figure 4**. Overall, ion channel mRNA levels were similar between the young and aged animals. Statistically (SAM test), none of the genes were expressed at lower levels in the aged samples, whereas seven (PMCA3, NCX3, SERCA1, Cavβ4, Cav2.3, sorcin and RyR1) were expressed at elevated mRNA levels.

We also investigated the effects of aging on K_{ATP} channel subunit protein expression (**Figure 5**). Membranes, isolated from the hearts of young and aged rats, subjected to SDS-PAGE, were immunoblotted with antibodies against Kir6.2, SUR1, SUR2A and SUR2B. These data demonstrated little alterations in K_{ATP} channel subunit expression in the aging rat heart.

Effects of K_{ATP} channel activity on action potentials: Numerical modeling

The reduced K_{ATP} channel current density and the increased ATP-sensitivity predict that K_{ATP} channel opening will have a lesser effect on action potential properties during metabolic impairment. We wanted to investigate the physiological consequences of these changes independent of the known age-related metabolic changes and alterations in other ionic currents (Walker *et al.* 1993). We therefore employed an empirical numerical model of the K_{ATP} channel, adapted from the Ferrero model (Ferrero *et al.* 1996), that we recently implemented to investigate K_{ATP} channels in the cardiac conduction system (Bao *et al.* 2011b). This model was adapted by incorporating relevant parameters to account for the K_{ATP} channel current density, unitary conductance and ATP-sensitivity that we measured in our experiments. We incorporated the K_{ATP} channel model into an action potential model of the human ventricle (ten Tusscher *et al.* 2004) and simulated the effects of decreasing the cytosolic ATP and ADP concentrations on action potential duration (**Figure 6**). Decreasing the ATP:ADP ratio progressively shortened the simulated APD from ~400ms to ~60ms. When adjusting the model to incorporate K_{ATP} channel parameters measured in the aged heart, the action potential duration shortening was less pronounced.

Discussion

Our data demonstrate that aging is associated with the reported electrophysiological alterations isolated cardiac myocytes, notably an increased action potential duration. The whole-cell K_{ATP} channel current density was significantly reduced in two animal models of aging. Measurements with isolated, inside-out, patches revealed a complex dependence of the K_{ATP} channel on cytosolic ATP, with an increased sensitivity to inhibitory ATP in the aged group. The mRNA or protein expression of K_{ATP} channel subunits was not affected by age. Numerical simulation studies predicted that K_{ATP} channel opening will be less likely to shorten the action potential upon metabolic impairment in the aged heart.

The Fischer 344 rat model

Comorbid diseases complicate the study of aging in humans and animal models are often used as a model of human aging (Institute of Laboratory Animal Resources (U.S.). Committee on Animal Models for Research on Aging 1981; Conn 2006). The Fischer 344/ Brown Norway F1 (F344/BNF1) rat is recommended by the National Institutes on Aging as a suitable model of age-related pathophysiological changes (Institute of Laboratory Animal Resources (U.S.). Committee on Animal Models for Research on Aging 1981). These hybrid rats live longer and have a lower rate of pathological conditions than inbred rats (Walker *et al.* 2006). The recommended age (when 50% mortality is achieved) is 24 and 26 months respectively for males and females of the Fischer 344 rat[1]. These animals develop

significant cardiac deficits, including arrhythmias, left ventricular (LV) dilation, mild hypertrophy, and depressed cardiac function (Walker *et al.* 2006). Consistent with the absence of hypertrophy, the cell capacitance (an index of the electrically active cell surface) was not different in isolated myocytes from hearts of young and aged Fischer rats. We also performed limited recordings using isolated ventricular myocytes from C57BL/6 mouse hearts. In this group, we found that the cell capacitance was larger in the aged group compared to the young group, which indicates the possibility of significant hypertrophy. This may, however, be related to a more advanced age since we studied these mice at ~29-30 months of age [the reported life expectancy in males of this strain is ~29 months (Kunstyr & Leuenberger 1975)].

Decreased K_{ATP} channel current density with aging

We found a significant decrease in the K_{ATP} channel currents that were activated by metabolic inhibition in the aged rat ventricular myocytes. This current density, corrected for cell size, was inhibited by glibenclamide and represents activation of the K_{ATP} channel (Bao *et al.* 2011a; Yoshida *et al.* 2011). This finding is consistent with a prior data that describe a decreased K_{ATP} channel current with aging (Ranki *et al.* 2002). However, the latter study reported that the K_{ATP} channel current decrease only occurs in the hearts of the female gender (Ranki *et al.* 2002), but not in males. In contrast, our data were obtained using male rats and mice. A possible explanation for the sex difference might be due to the species being used (we used rodent models, whereas Ranki et al (Ranki *et al.* 2001) used guinea pigs). It must also be noted that the guinea pigs were studied at a much younger comparative age (they studied 18 month old animals, whereas survival analysis of guinea pigs shows 50% mortality at ~30 months for females and ~45 months for males (Institute of Laboratory Animal Resources (U.S.). Committee on Animal Models for Research on Aging 1981)) and it is possible that K_{ATP} channel current differences would also be observed in male guinea pigs if studied at a later age).

The mechanism of K_{ATP} channel current decrease

Our studies do not provide a direct insight into the mechanism(s) by which the K_{ATP} channel density is decreased in the aged heart. In contrast to a previous report that used middle-aged (18 month-old) guinea pigs (Ranki *et al.* 2002), we did not observe significant alterations in mRNA expression of the K_{ATP} channel subunits. When extending the assay to incorporate a large number (>80) of subunits of ion channels, regulatory subunits, exchangers and pumps, with a few exceptions we similarly found their mRNA levels not to differ between young and aged hearts. This occurred despite significant age-related alterations in electrophysiological properties (**Figure 1**) (Walker *et al.* 1993) and intracellular Ca^{2+} signalling (Howlett 2010). Thus, in general, ion channels appear to be under the control of post-transcriptional regulatory mechanisms in the aging heart. Our Western blots indicate that total protein expression of K_{ATP} channel subunits is unchanged in the aged heart. We recently described that a large percentage of ventricular K_{ATP} channels are found in intracellular (endosomal) compartments from which the surface pool of K_{ATP} channels can be replenished by endocytic recycling mechanisms (Bao *et al.* 2011a). How this process and possible post-translational modifications contribute to the decreased K_{ATP} channel surface density observed in the present studies will be investigated in future experiments.

[1] http://www.nia.nih.gov/ResearchInformation/ScientificResources/AgedRodentColoniesHandbook/StrainSurvivalInformation.htm

Alterations in K_{ATP} channel nucleotide sensitivity with aging

A prototypical feature of K_{ATP} channels is their block by intracellular ATP and activation by MgADP (Nichols 2006). The nucleotide-sensitivity of K_{ATP} channels determine their functional roles during metabolic alterations. Changes in ventricular K_{ATP} channel ATP-sensitivity have previously been documented in conditions such as diabetes (Shimoni *et al.* 1998), hypertrophy (Cameron *et al.* 1988) and hypothyroidism (Light *et al.* 1998) but the underlying mechanisms and the structural correlates of the altered ATP-sensitivities remain to be established. The ATP-sensitivity of K_{ATP} channels also differs depending on their tissue distribution, for example as we recently reported for the K_{ATP} channel of the specialized cardiac conduction system (Bao *et al.* 2011b). Typically, the ATP-sensitivity of K_{ATP} channels is well described by a modified Hill function, which describes a sigmoidal relationship that is determined by the ATP concentration at which half-maximal inhibition occurs and by a factor (Hill coefficient) that describes the steepness of this relationship. The IC_{50} value in rat ventricular myocytes is normally described to be between 25-80 μM (Lederer & Nichols 1989; Light *et al.* 1998). We found the K_{ATP} channels in the aged group to be highly sensitive to inhibitory ATP. However, the ATP dose-response curve could not be simply described by a single Hill function and we needed to use a sum of two Hill functions to describe the data, suggesting the possibility that ATP mediates its effect through both low (low micromolar) and higher affinity binding. Although the data in the young group can adequately be described by single affinity model, they can better described by a biphasic affinity model (see Supplemental file). When using the biphasic model, the ATP IC_{50} values and Hill coefficients were similar in the young and aged groups, suggesting that ATP-binding was not affected. In contrast, the relative contributions of the low and high affinity components were different, with the high-affinity component dominating in the aged group. From structural perspectives, it is unlikely that K_{ATP} channel has two separate ATP-binding sites (Nichols 2006). Thus, the most parsimonious explanation of our data is to assume the presence of two separate pools of K_{ATP} channels with distinct ATP-sensitivities, possibly caused by different combinations of K_{ATP} channel subunits or resulting from post-translational modifications.

Effects of K_{ATP} channel opening

The effects of K_{ATP} channel opening on the action potential in the aging ventricular myocyte will depend on several factors, including the contributions of other ion channel activities (Lakatta *et al.* 1975; Lakatta & Yin 1982; Howlett 2010), as well as altered metabolic (Johnson & Hammer 1993) and oxidative status (Dai & Rabinovitch 2009) of the aged heart. To eliminate these confounding factors, we performed a numerical simulation of the 'normal' human ventricular action potential (ten Tusscher *et al.* 2004) and incorporated a model of the ventricular K_{ATP} channel to investigate the effects of decreased cytosolic ATP levels (and subsequent activation of K_{ATP} channels). When incorporating model with parameters that match the K_{ATP} channel properties measured in the aged group (smaller current density and increased ATP sensitivity), the simulated action potential was less sensitive to decreases of cytosolic ATP. At face value, this result would argue that K_{ATP} channels are less likely to be activated during cardiac ischemia and hence may have a lesser protective role in the aged heart. Data regarding the effects of aging on infarct size are mixed. In rats, there is evidence of increased injury with aging (Ananthakrishnan *et al.* 2011). There is also evidence that both preconditioning and post-conditioning are impaired in the aged heart (Boengler *et al.* 2009). The role of the K_{ATP} channel in these processes remains to be investigated. A recent study demonstrated that glycolytic inhibition (replacing glucose with pyruvate) causes spontaneous ventricular fibrillation in aged rat hearts (Morita *et al.* 2011). Moreover, these arrhythmias were suppressed by the K_{ATP} channel blocker glibenclamide. Since K_{ATP} channel subunits associate with glycolytic enzymes and the

activity of glycolytic enzymes regulate the function of K_{ATP} channels (Hong *et al.* 2011), it will be a priority to investigate this mode of regulation of K_{ATP} channels in the aged heart.

Significance

Aging is known to take a toll on the well-being of an individual with heart being a major organ affected by age. Several studies suggest a high degree of incidence of heart failure and related deaths associated with aging. The cardio-protective role of K_{ATP} channels in aging individuals is still unclear. Though our data suggest a possible decrease in channel density and function, further research is necessary to determine the role of decreased K_{ATP} channels in aging. This research could assist in a better understanding of aging heart physiology and designing means to improve cardiac health in aging individuals.

Supplementary Material

Refer to Web version on PubMed Central for supplementary material.

Acknowledgments

None.

FUNDING

This work was supported by National Institutes of Health grants HL105046 to LB, P01AG026467 to AMS and RR and HL085820 & HL093563 to WAC.

REFERENCES

Ananthakrishnan R, Li Q, Gomes T, Schmidt AM, Ramasamy R. Aldose reductase pathway contributes to vulnerability of aging myocardium to ischemic injury. Exp Gerontol. 2011; 46:762–767. [PubMed: 21600277]

Andersen CL, Jensen JL, Orntoft TF. Normalization of real-time quantitative reverse transcription-PCR data: a model-based variance estimation approach to identify genes suited for normalization, applied to bladder and colon cancer data sets. Cancer Research. 2004; 64:5245–5250. [PubMed: 15289330]

Bao L, Hadjiolova K, Coetzee WA, Rindler MJ. Endosomal KATP channels as a reservoir after myocardial ischemia: a role for SUR2 subunits. Am J Physiol Heart Circ Physiol. 2011a; 300:H262–270. [PubMed: 20971764]

Bao L, Kefaloyianni E, Lader J, Hong M, Morley G, Fishman GI, Sobie EA, Coetzee WA. Unique properties of the ATP-sensitive K^+ channel in the mouse ventricular cardiac conduction system. Circ Arrhythm Electrophysiol. 2011b; 4:926–935. [PubMed: 21984445]

Boengler K, Schulz R, Heusch G. Loss of cardioprotection with ageing. Cardiovasc Res. 2009; 83:247–261. [PubMed: 19176601]

Cameron JS, Kimura S, Jackson-Burns DA, Smith DB, Bassett AL. ATP-sensitive K^+ channels are altered in hypertrophied ventricular myocytes. American Journal of Physiology. 1988; 255:H1254–H1258. [PubMed: 2847560]

Conn, PM. Handbook of models for human aginged^eds). Elsevier Academic Press; Amsterdam: 2006.

Dai DF, Rabinovitch PS. Cardiac aging in mice and humans: the role of mitochondrial oxidative stress. Trends Cardiovasc Med. 2009; 19:213–220. [PubMed: 20382344]

Ferrero JM Jr. S iz J, Ferrero JM, Thakor NV. Simulation of action potentials from metabolically impaired cardiac myocytes - Role of ATP-sensitive K + current. Circulation Research. 1996; 79:208–221. [PubMed: 8755997]

Fleg, JLLE. Normal aging of the cardiovascular system.. In: Aronow, WS.; Fleg, JL., editors. Cardiovascular disease in elderly. 4th edn. Informa Healthcare USA Inc.; New York: 2008. p. 1-43.

Fleg JL, Strait J. Age-associated changes in cardiovascular structure and function: a fertile milieu for future disease. Heart Fail Rev. 2011

Gross GJ, Peart JN. KATP channels and myocardial preconditioning: an update. Am.J.Physiol Heart Circ.Physiol 2003.Sep.;285.(3):H921.-30. 2003; 285:H921–H930.

Harrell MD, Harbi S, Hoffman JF, Zavadil J, Coetzee WA. Large-scale analysis of ion channel gene expression in the mouse heart during perinatal development. Physiol Genomics. 2007; 28:273–283. [PubMed: 16985003]

Hong M, Kefaloyianni E, Bao L, Malester B, Delaroche D, Neubert TA, Coetzee WA. Cardiac ATP-sensitive K^+ channel associates with the glycolytic enzyme complex. FASEB J. 2011; 25:2456–2467. [PubMed: 21482559]

Howlett SE. Age-associated changes in excitation-contraction coupling are more prominent in ventricular myocytes from male rats than in myocytes from female rats. Am J Physiol Heart Circ Physiol. 2010; 298:H659–670. [PubMed: 19966062]

Huang X, Yang P, Du Y, Zhang J, Ma A. Age-related down-regulation of HCN channels in rat sinoatrial node. Basic Research in Cardiology. 2007; 102:429–435. [PubMed: 17572839]

Institute of Laboratory Animal Resources (U.S.). Mammalian Models for Research on Aging. National Academies Press; Washington, D.C.: 1981. Committee on Animal Models for Research on Aging A.

Johnson P, Hammer JL. Cardiac and skeletal muscle enzyme levels in hypertensive and aging rats. Comp Biochem Physiol B. 1993; 104:63–67. [PubMed: 8448994]

Kunstyr I, Leuenberger HG. Gerontological data of C57BL/6J mice. I. Sex differences in survival curves. J Gerontol. 1975; 30:157–162. [PubMed: 1123533]

Lakatta EG, Gerstenblith G, Angell CS, Shock NW, Weisfeldt ML. Prolonged contraction duration in aged myocardium. J Clin Invest. 1975; 55:61–68. [PubMed: 1109181]

Lakatta EG, Yin FC. Myocardial aging: functional alterations and related cellular mechanisms. Am J Physiol. 1982; 242:H927–941. [PubMed: 6283905]

Lederer WJ, Nichols CG. Nucleotide modulation of the activity of rat heart ATP-sensitive K^+ channels in isolated membrane patches. Journal of Physiology (London). 1989; 419:193–211. [PubMed: 2621629]

Light P, Shimoni Y, Harbison S, Giles W, French RJ. Hypothyroidism decreases the ATP sensitivity of K ATP channels from rat heart. Journal of Membrane Biology. 1998; 162:217–223. [PubMed: 9543494]

Liu SJ, Wyeth RP, Melchert RB, Kennedy RH. Aging-associated changes in whole cell K^+ and L-type Ca^{2+} currents in rat ventricular myocytes. Am J Physiol Heart Circ Physiol. 2000; 279:H889–900. [PubMed: 10993747]

Morita N, Lee JH, Bapat A, Fishbein MC, Mandel WJ, Chen PS, Weiss JN, Karagueuzian HS. Glycolytic Inhibition Causes Spontaneous Ventricular Fibrillation in Aged Hearts. Am J Physiol Heart Circ Physiol. 2011

Morrissey A, Parachuru L, Leung M, Lopez G, Nakamura TY, Tong X, Yoshida H, Srivastiva S, Chowdhury PD, Artman M, Coetzee WA. Expression of ATP-sensitive K+ channel subunits during perinatal maturation in the mouse heart. Pediatric Research. 2005; 58:185–192. [PubMed: 16085792]

Nichols CG. K_{ATP} channels as molecular sensors of cellular metabolism. Nature. 2006; 440:470–476. [PubMed: 16554807]

Poole LB, Maw-Shung L, Landfield PW. Kinetic studies of the Na^+-K^+-ATPase enzyme system in brain and heart of the aging rats. American Journal of Physiology. 1984; 247:R850–R855. [PubMed: 6093604]

Ranki HJ, Budas GR, Crawford RM, Jovanovic A. Gender-specific difference in cardiac ATP-sensitive K^+ channels. J.Am.Coll.Cardiol. 2001; 38:906–915. [PubMed: 11527652]

Ranki HJ, Crawford RM, Budas GR, Jovanovic A. Ageing is associated with a decrease in the number of sarcolemmal ATP-sensitive K+ channels in a gender-dependent manner. Mech Ageing Dev. 2002; 123:695–705. [PubMed: 11850031]

Rosen MR, Reder RF, Hordof AJ, Davies M, Danilo P Jr. Age-related changes in Purkinje fiber action potentials of adult dogs. Circulation Research. 1978; 43:931–938. [PubMed: 709754]

Rumberger E, Timmermann J. Age-changes of the force-frequency-relationship and the duration of action potential of isolated papillary muscles of guinea pig. Eur J Appl Physiol Occup Physiol. 1976; 35:277–284. [PubMed: 976255]

Seino S, Miki T. Physiological and pathophysiological roles of ATP-sensitive K+ channels. Prog Biophys Mol Biol. 2003; 81:133–176. [PubMed: 12565699]

Shimoni Y, Light PE, French RJ. Altered ATP sensitivity of ATP-dependent K^+ channels in diabetic rat hearts. American Journal of Physiology. 1998; 275:E568–E576. [PubMed: 9755074]

ten Tusscher KH, Noble D, Noble PJ, Panfilov AV. A model for human ventricular tissue. Am J Physiol Heart Circ Physiol. 2004; 286:H1573–1589. [PubMed: 14656705]

Tricarico D, Camerino DC. ATP-sensitive K^+ channels of skeletal muscle fibers from young adult and aged rats: possible involvement of thiol-dependent redox mechanisms in the age-related modifications of their biophysical and pharmacological properties. Molecular Pharmacology. 1994; 46:754–761. [PubMed: 7969056]

Walker EM Jr. Nillas MS, Mangiarua EI, Cansino S, Morrison RG, Perdue RR, Triest WE, Wright GL, Studeny M, Wehner P, Rice KM, Blough ER. Age-associated changes in hearts of male Fischer 344/Brown Norway F1 rats. Ann Clin Lab Sci. 2006; 36:427–438. [PubMed: 17127729]

Walker KE, Lakatta EG, Houser SR. Age associated changes in membrane currents in rat ventricular myocytes. Cardiovascular Research. 1993; 27:1968–1977. [PubMed: 8287405]

Yoshida H, Bao L, Kefaloyianni E, Taskin E, Okorie U, Hong M, Dhar-Chowdhury P, Kaneko M, Coetzee WA. AMP-activated protein kinase connects cellular energy metabolism to K(ATP) channel function. J Mol Cell Cardiol. 2011

Yoshida H, Feig J, Ghiu IA, Artman M, Coetzee WA. K(ATP) channels of primary human coronary artery endothelial cells consist of a heteromultimeric complex of Kir6.1, Kir6.2, and SUR2B subunits. Journal of Molecular and Cellular Cardiology. 2004; 37:857–869. [PubMed: 15380676]

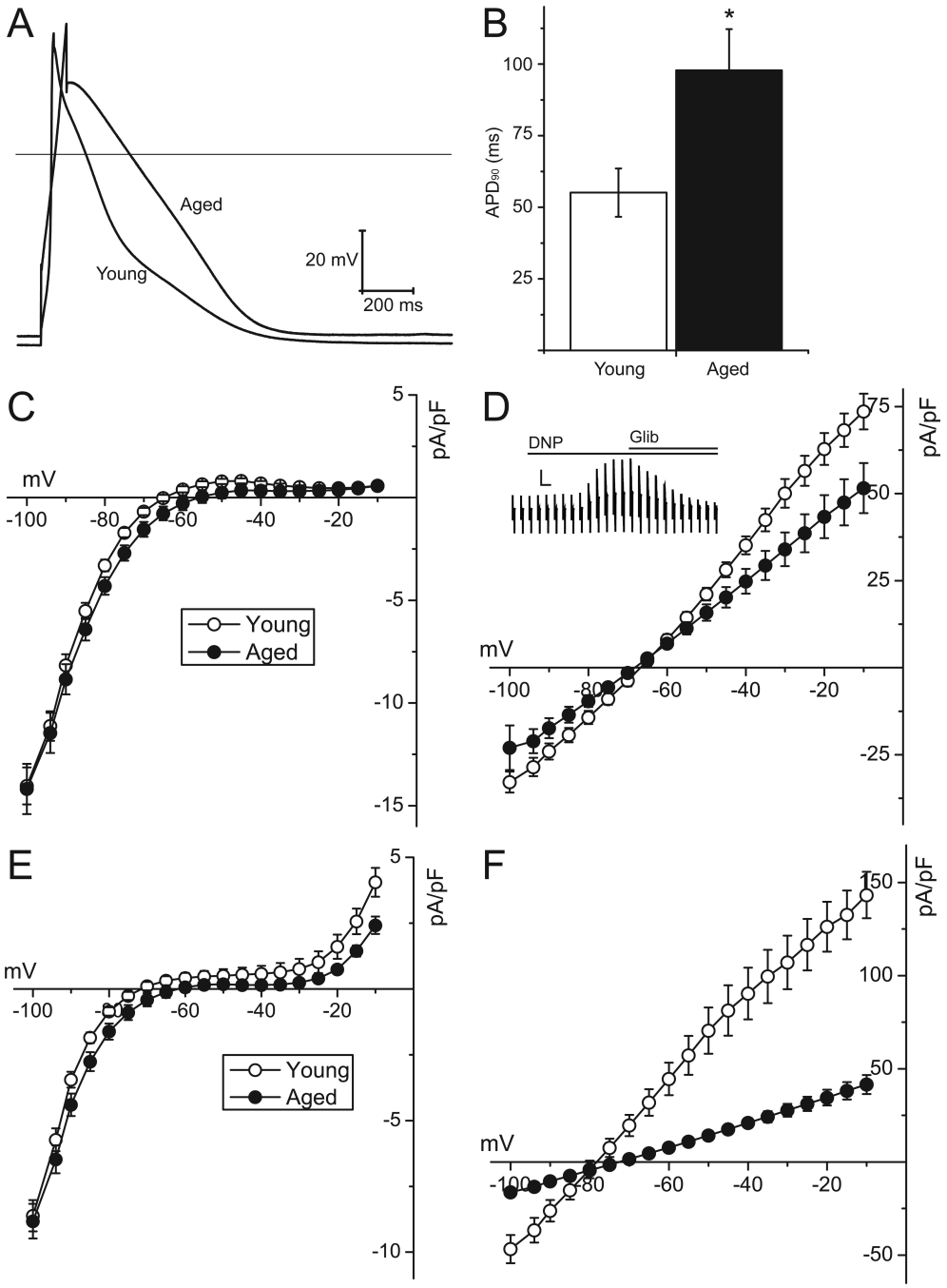

Figure 1. Action potential configuration and whole-cell K_{ATP} channel density are altered in the aged myocytes compared to young rat ventricular myocytes

A) Representative whole-cell action potentials, evoked by current injection at 1Hz through the patch pipette, in ventricular myocytes isolated from young or aged rats. The horizontal line represents zero voltage. B) Summary data of the action potential duration, recorded at 90% repolarization (APD_{90}), of young (n=14 cells from 3 animals) and aged (n=17 cells from 3 animals) ventricular myocytes. *p<0.0; Mann-Whitney Rank Sum test. C) Current-voltage relationships obtained under normoxic conditions using a ramp voltage protocol (5 to -100 mV; ramp rate of -25 $mV \cdot s^{-1}$, applied every 20s from a holding potential of -45 mV). The input resistances were 7.98 ± 0.86 MΩ in aged rats and 6.54 ± 0.71 MΩ in young rats.

Data are shown for young (open symbols) and aged (filled symbols) rat ventricular myocytes. D) Current-voltage relationships obtained after application of 2.4-dinitrophenol (DNP, 100 μM). Currents are expressed as current density (pA/pF). The inset shows a representative current trace recorded from a ventricular myocyte. The scale bar represents 4 nA and 20 s. E) Normoxic current-voltage relationships in young and aged mouse ventricular myocytes. F) Current-voltage relationships in mouse ventricular myocytes after application of DNP (100 μM). The cell capacitance was smaller in the young mouse ventricular myocytes (147.6±12.4, n=14) compared to the aged myocytes (197.6±11.7; n=14; p= 0.007, Student's t-test).

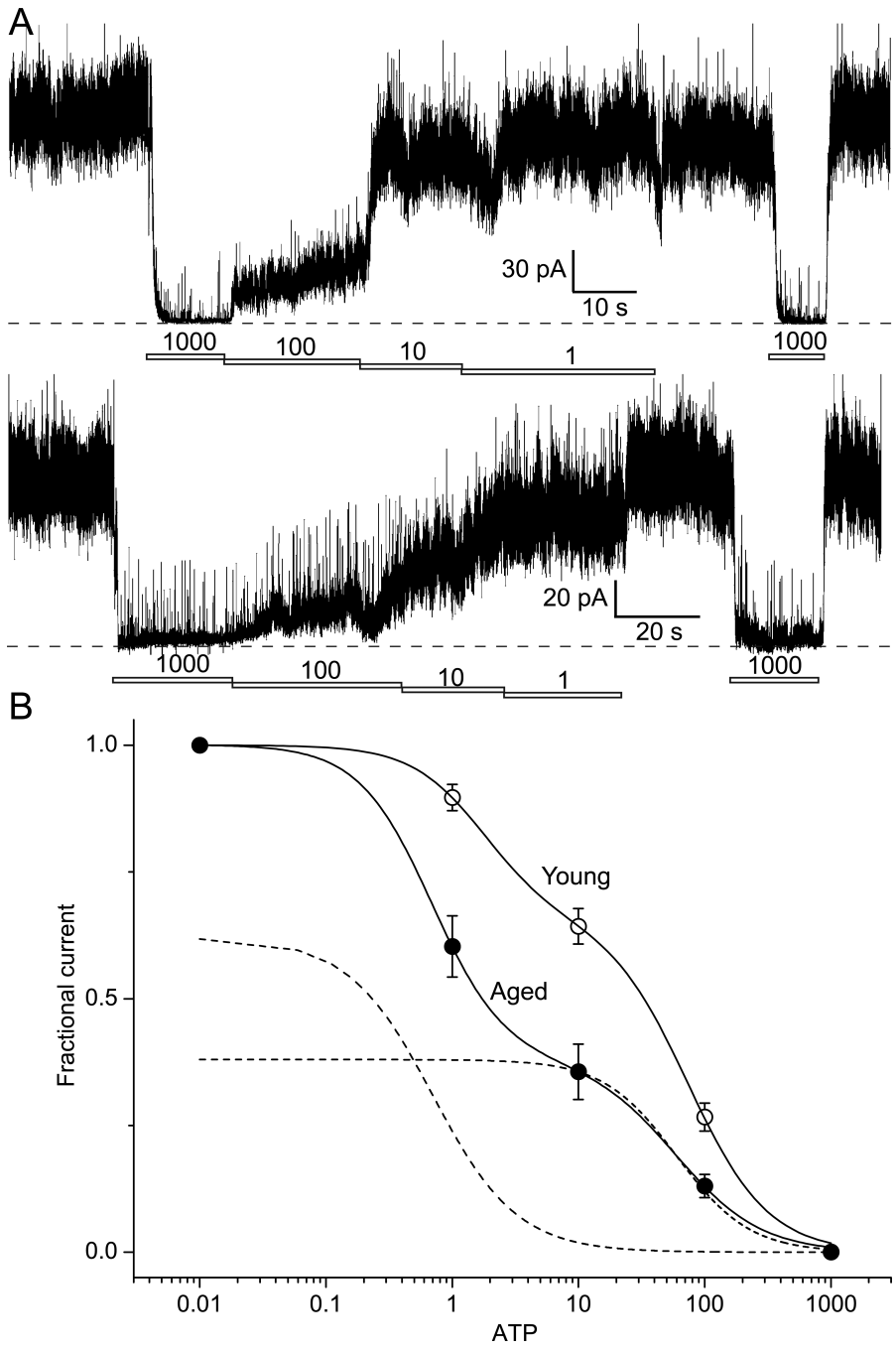

Figure 2. Effects of age on nucleotide sensitivity of cardiac K_{ATP} channels

A) Patch clamp current recordings, made in the inside-out configuration, obtained from isolated ventricular myocytes of young (top trace) and aged (bottom trace) rat hearts. The ATP concentrations were changed as indicated. The dashed line represents zero current. B) The fractional current (mean patch current divided by the current recorded in the absence of ATP) is plotted as a function of the ATP concentrations. The data points are means and SEM for young (open symbols; n=20 patches from 3 animals) and aged (filled symbols; n=16 patches from 3 animals) groups. These data were subjected to curve fitting to a sum of two modified Hill equations (see Methods section for equations). The solid lines represent the result of the curve fitting. The two dotted lines represent the low- and high-sensitivity

components of the ATP-sensitivity curve of the aged group. The IC_{50} values, Hill coefficients and weights of the components are provided in the text.

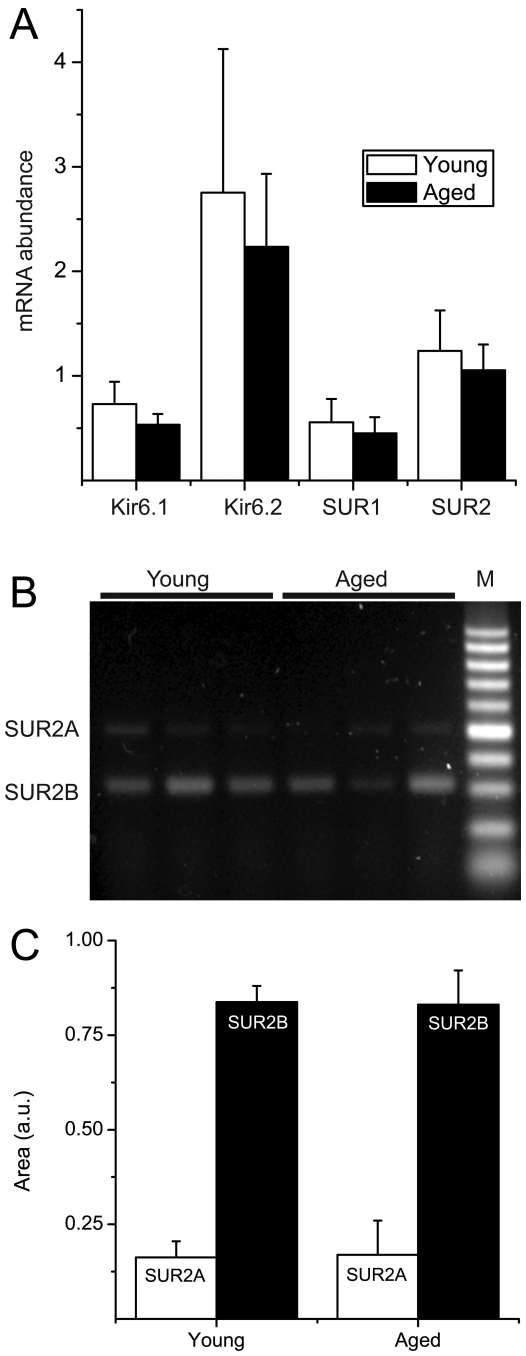

Figure 3. K_{ATP} channel subunit mRNA expression in rat aged and young ventricular myocytes

A) semi-quantitative real-time RT-PCR data showing mRNA expression of rat Kir6.1, Kir6.2, SUR1 and SUR2 subunits in total RNA extracted from young (n=5) or aged (n=5) rat ventricles. Data are expressed relative to that of β-actin. B) Conventional RT-PCR was performed to discriminate between SUR2 spice variants expressed in ventricular myocytes isolated from young or aged rat hearts. A primer pair was used that resulted in a 493 bp amplicon for SUR2A and a 317 bp band for SUR2B. The PCR products were sequenced to confirm the identity of the amplicons. C) Bar graph depicting the relative expression of SUR2A or SUR2B (n=4 animals in each group). There were no significant age-dependent differences in these transcripts.

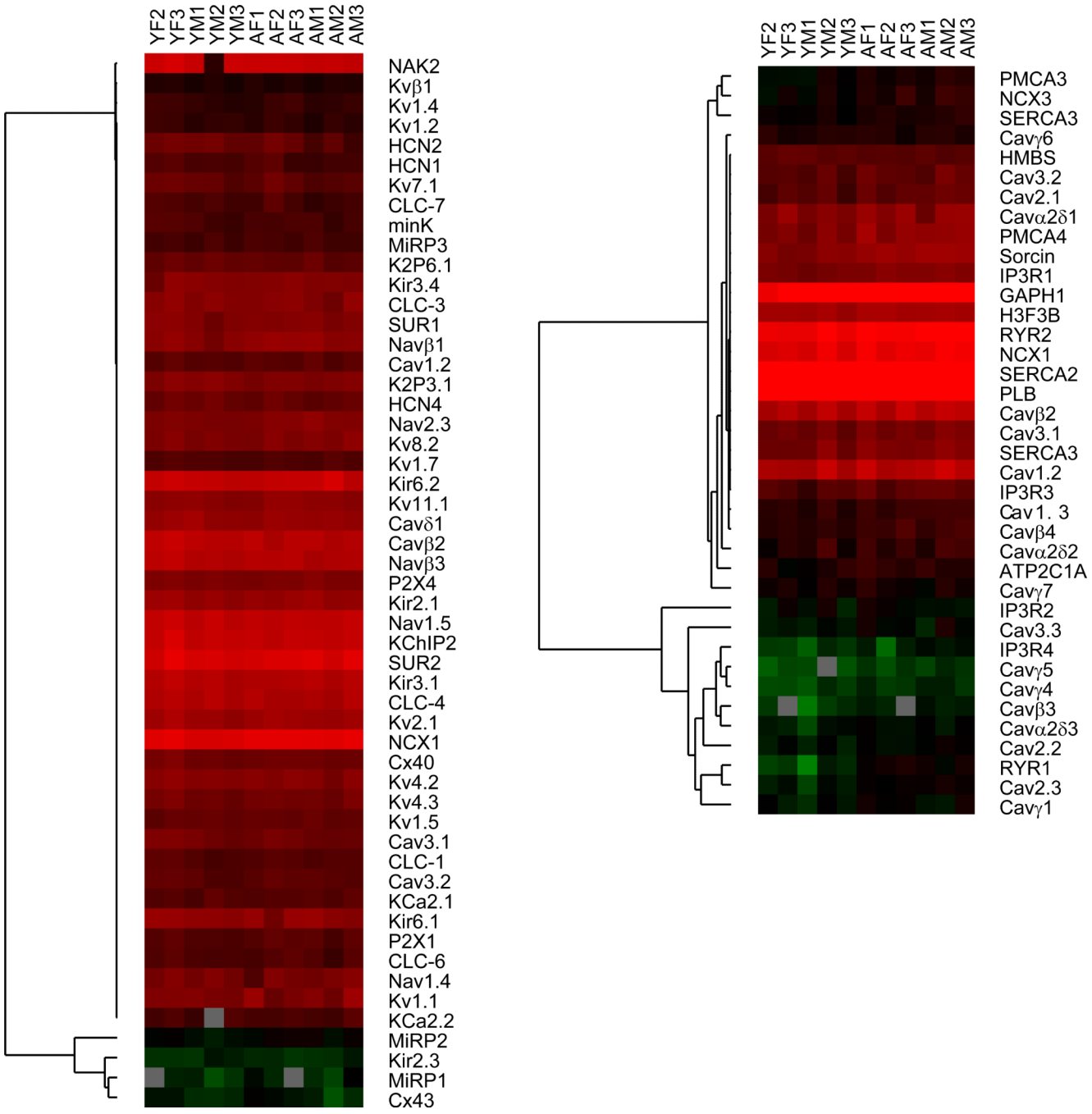

Figure 4. Lack of transcriptional regulation of ion channel genes with aging

Real-time RT-PCR was performed using primers specific to eighty two ion subunits of ion channels, pumps or exchangers, using RNA isolated from young male or female (n=3 each) or aged male or female (n=3 each) hearts. Data were analyzed relative to the average expression of the following reference genes: hydroxymethylbilane synthase, histone H3 and cyclophilin B. Hierarchical clustering was performed after $\log_2$ transformation (no other data adjustments or normalization was performed) and visualized as a heat map using MEV.

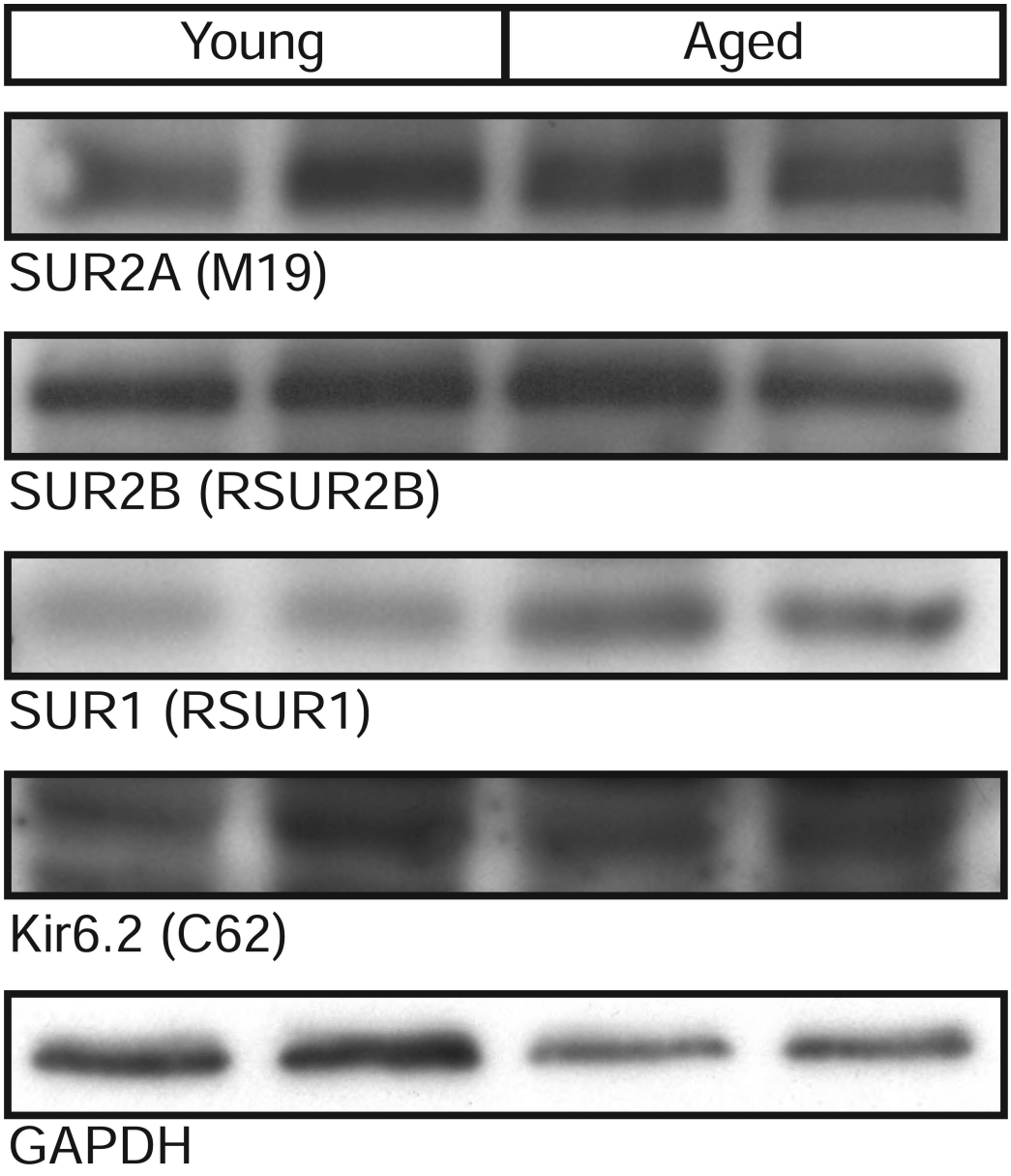

Figure 5. K_{ATP} channel subunit protein expression in young and aged rat hearts

Membrane preparations from young or aged rat hearts were subjected to 10% SDS-PAGE and immunoblotted with antibodies against Kir6.2, SUR1, SUR2A, SUR2B or GAPDH.

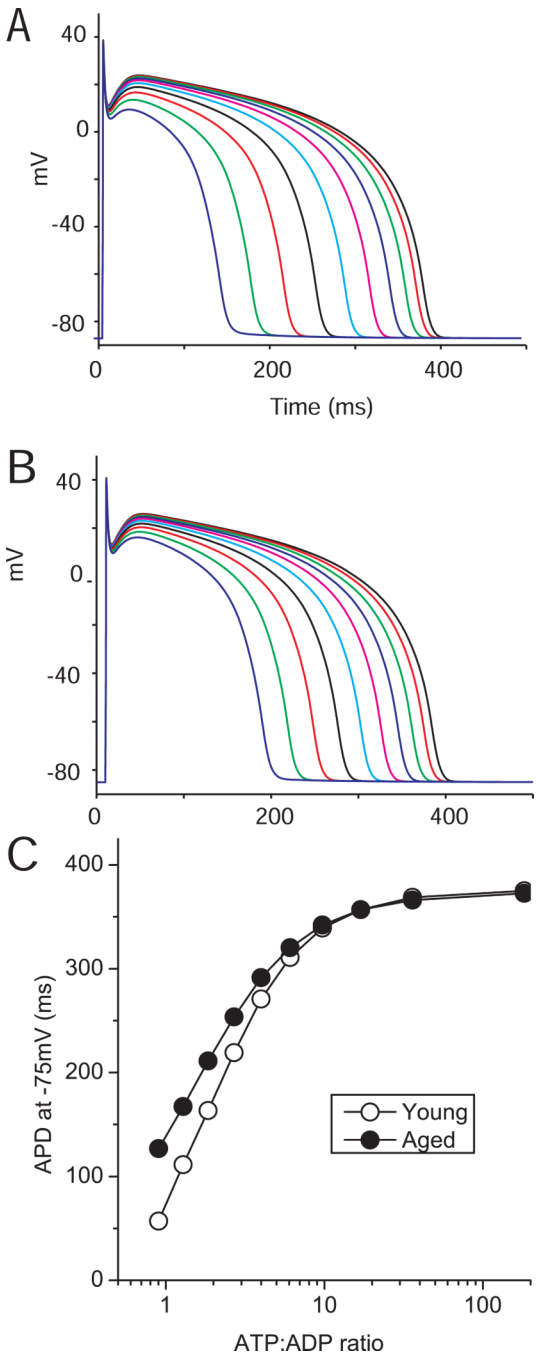

Figure 6. Simulating the effects of K_{ATP} channel opening on action potential duration

The ten Tusscher human ventricular action potential model (ten Tusscher *et al.* 2004) was used to incorporate a K_{ATP} channel simulation (Ferrero *et al.* 1996; Bao *et al.* 2011b). Action potentials were simulated with 6.3, 5.1, 4.2, 3.4, 2.8, 2.3, 1.8, 1.5, 1.2 and 1 mM ATP using K_{ATP} channel parameters determined from A) young and B) aged Fischer 344 rat hearts. We simultaneously adjusted ADP to pathophysiologically relevant levels. Since most cellular ADP is bound (e.g. to actin), the free ADP level was estimated to be 5% of the total nucleotide concentration (assumed to be 7mM) minus the ATP concentration (e.g. 35, 95, 140, 180, 210, 235, 260, 275, 290 and 300 μM). C) The action potential duration (measured at -75 mV) is plotted as a function of the ATP:ADP ratio. Note that the action potential

properties themselves were not adjusted for age to more accurately examine effects of K_{ATP} channel opening.

Table 1

Primers used for K_{ATP} channel subunit mRNA expression.

Subunit	Forward		Reverse	
Kir6.1	5012F	5′-GAAAGGCATCACGGAGAAGA-3′	5012R	5′-CTCCAAACCCAATGGTCACT- 3′
Kir6.2	5013F	5′-CCTCCTATCTGGCTGACGAG-3′	5013R	5′-GTGGGCACTTTAACGGTGTT-3′
SUR1	5034F	5′-TCCAGAAGGTGGTGATGACA- 3′	5034R	5′-AGGTCTGCACTCAGGATGGT-3′
SUR2	5031F	5′-GCCTTTGTTCGAAAGAGCAG-3′	5031R	5′-GCTGTCATGACTACTTTCTGCAA-3′
SUR2A/B	1593F	5′-AATGCAAGTGCACAGACGAC-3′	1593R	5′-CAGGTCAGCAGTCAGAATGG-3′
β-actin	5000F	5′-AGATTACTGCCCTGGCTCCT-3′	5000R	5′-TAGAGCCACCAATCCACACA-3′

All primers are specific to rat sequences. The SUR2A/B primer pair was used for conventional RT-PCR; all others were used for real-time RT-PCR.

Table 2

Fitting parameters of ATP-sensitivity data

		Young	Aged
Single affinity model	IC_{50}	22.06	2.73
	Hill	0.752	0.54
Double affinity model	Amplitude	0.34	0.62
	IC_{50}	1.77	0.69
	Hill	1.5	1.5
	Amplitude	0.66	0.38
	IC_{50}	74.5	58.8
	Hill	1.4	1.4

The ATP sensitivity data obtained from patches of young or aged ventricular myocytes were fitted to a modified Hill equation to obtain the IC_{50} and Hill constant (slope). Alternatively, the data were subjected to curve fitting to a double affinity model, which is a sum of two Hill equations (see Methods).